Electronic Supplementary Material (ESI) for Journal of Materials Chemistry A.

Supporting Information

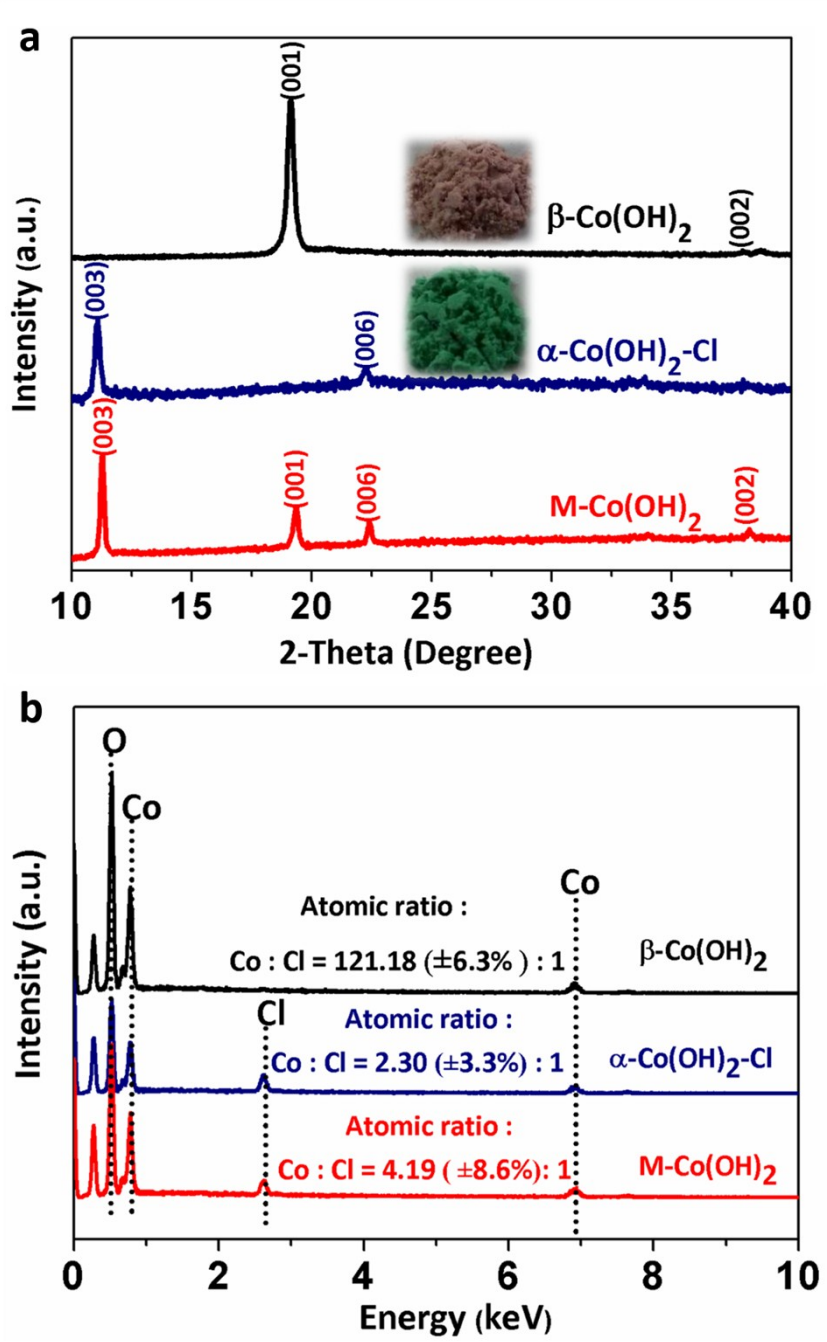

Figure S1. (a) XRD spectra of β-$Co(OH)_2$, α-$Co(OH)_2$-Cl and M-$Co(OH)_2$. The predominant 00*l* reflections of α- and β-phase are indicated as subscripts α and β, respectively. Insets of (a): the pink powders represent β-$Co(OH)_2$ and the green powders represent α-$Co(OH)_2$-Cl. (b) EDX spectra of β-$Co(OH)_2$, α-$Co(OH)_2$-Cl and M-$Co(OH)_2$, revealing different atomic ratios of Co : Cl.

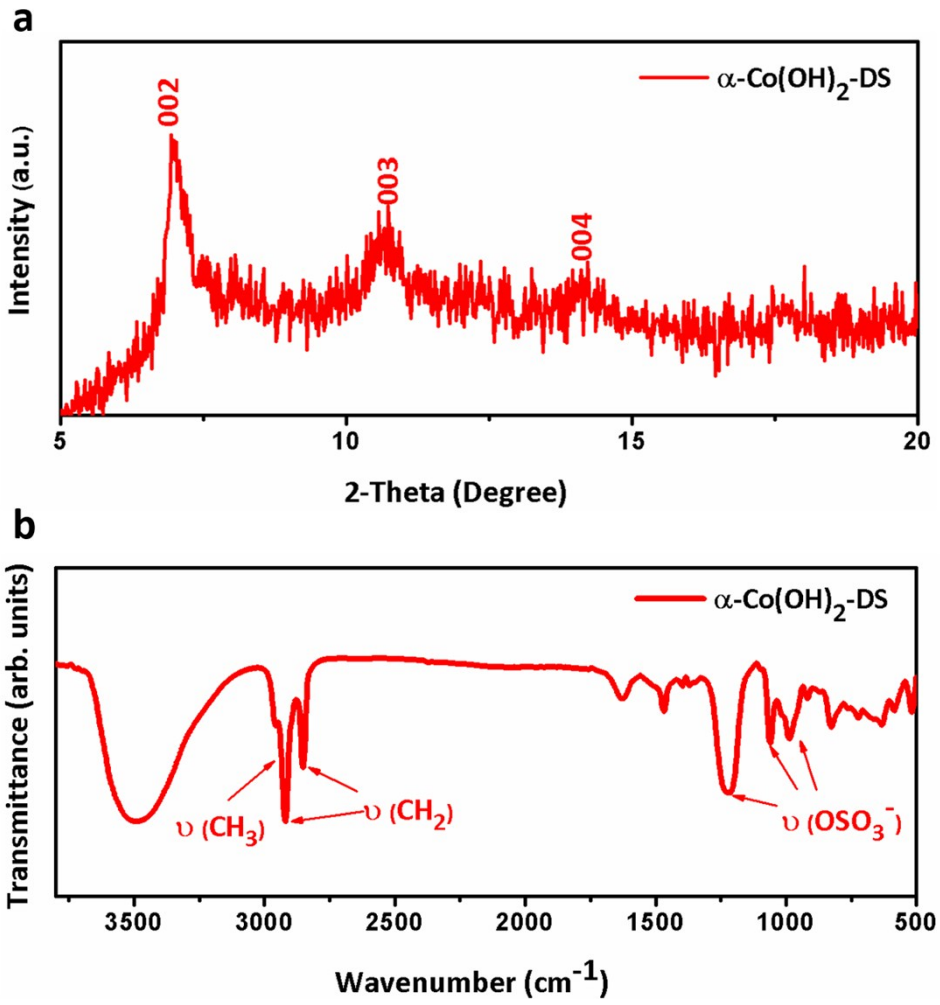

Figure S2. (a) XRD pattern of α-$Co(OH)_2$-DS, identifying the structure of α-type $Co(OH)_2$. (b) FT-IR spectrum of α-$Co(OH)_2$-DS, confirming the existence of dodecyl sulfate interlayer ions.

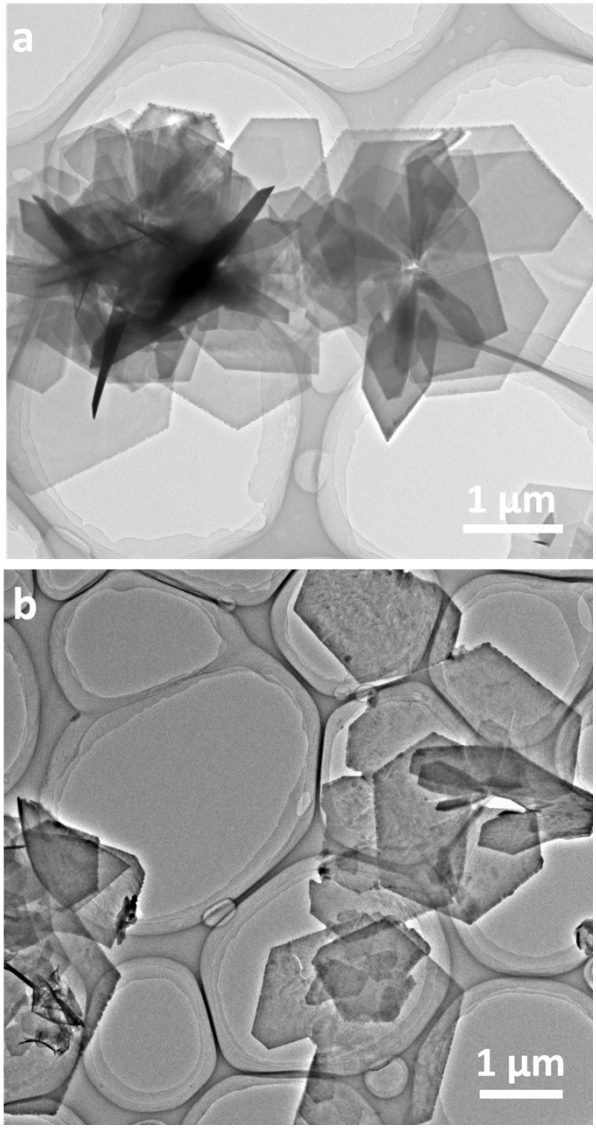

Figure S3. TEM images of α-$Co(OH)_2$-Cl (a) before OER test and (b) after OER test.

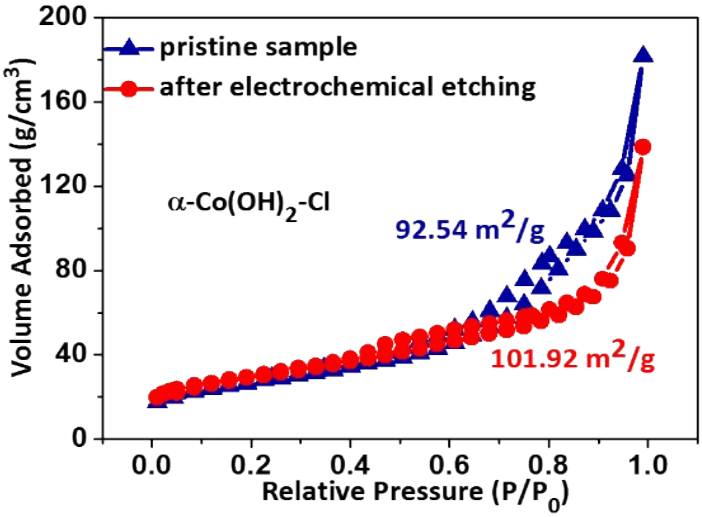

Figure S4. N_2 sorption isotherms of pristine and electrochemical etched α-$Co(OH)_2$-Cl.

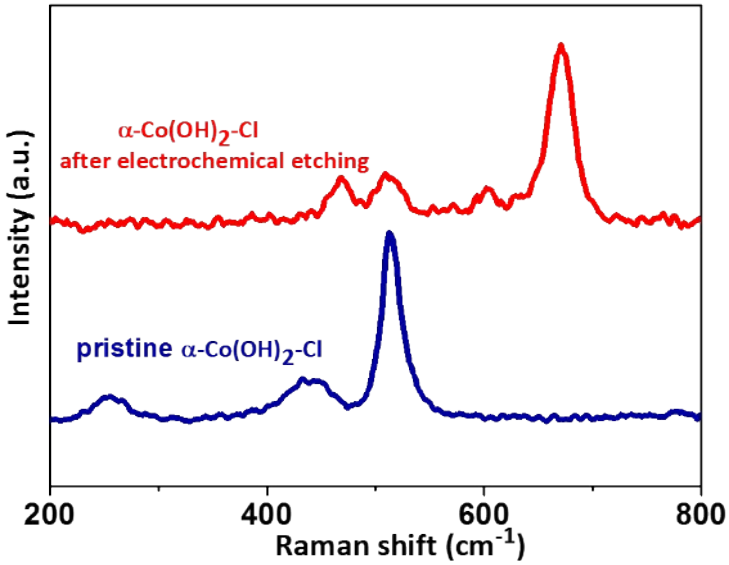

Figure S5. Raman spectra for the sample of α-$Co(OH)_2$-Cl before and after OER electrolysis in 1.0 M KOH.

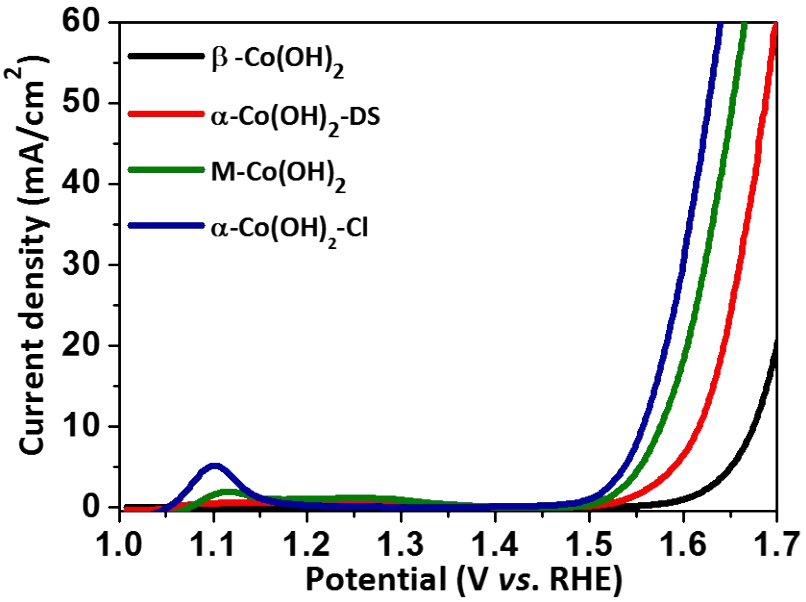

Figure S6. The polarization curves of β-$Co(OH)_2$, α-$Co(OH)_2$-DS, M-$Co(OH)_2$ and α-$Co(OH)_2$-Cl, respectively.

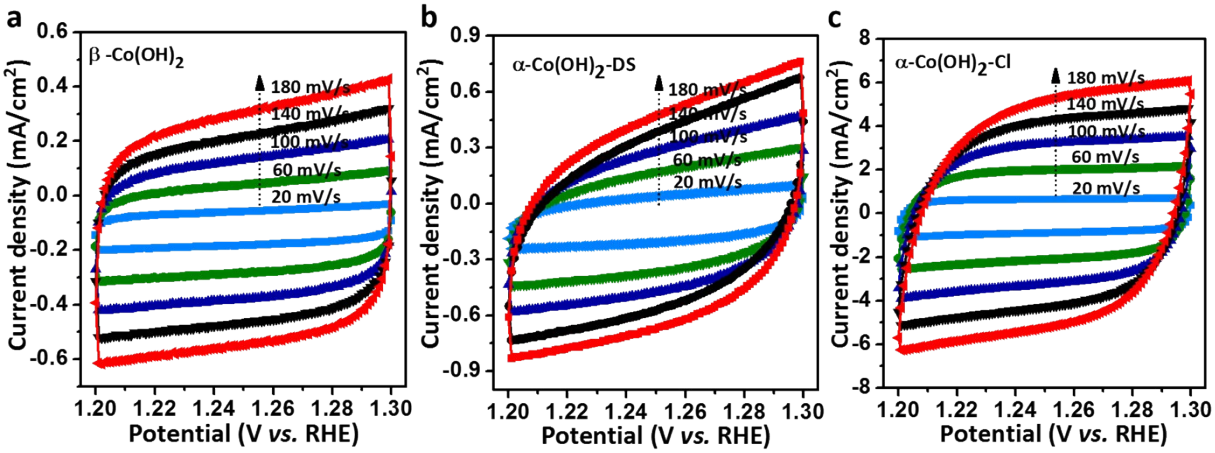

Figure S7. CVs at different scan rates in a potential window where no Faradaic processes occur (1.20 V ~ 1.30 V *vs.* RHE) for (a) β-$Co(OH)_2$, (b) α-$Co(OH)_2$-DS and (c) α-$Co(OH)_2$-Cl, respectively.

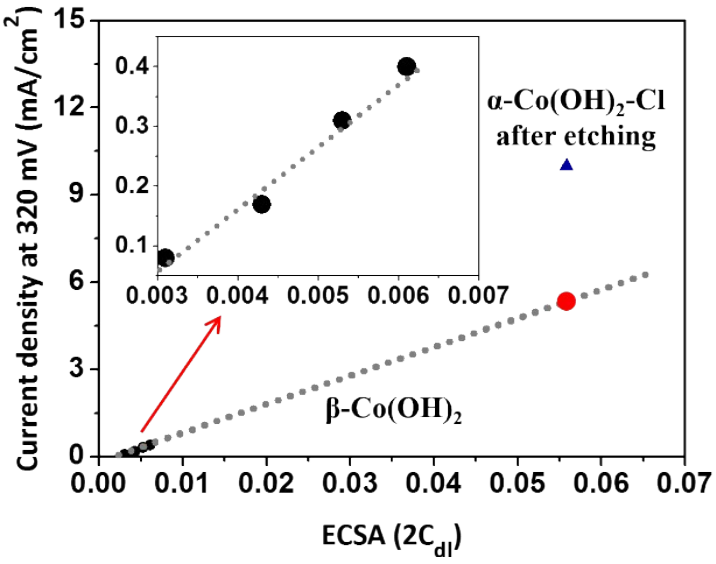

Figure S8. Current density at η = 320 mV plotted against ECSA for the sample of β-$Co(OH)_2$. Black solid sphere: β-$Co(OH)_2$ at different loadings; royal blue triangle: α-$Co(OH)_2$-Cl; red solid sphere: estimated activity of β-$Co(OH)_2$ with the same ECSA as α-$Co(OH)_2$-Cl.

Table S1. Comparison of ECSA and OER performance of α-$Co(OH)_2$-Cl and β-$Co(OH)_2$.

$ECSA_\alpha/ECSA_\beta$	j_α/j_β at η = 300 mV	j_α/j_β at η = 320 mV
12.98	44.44	58.82

Table S2. Comparison of selected recently reported Co-based OER electrocatalysts in the basic electrolyte.

Catalysts (mg/cm^2)	Electrolyte	Onset potential (mV)	Overpotential at 10 mA/cm^2 (mV)	Tafel slope (mV/decade)	References
Co_3O_4/C nanowires/Cu foil[a] (~0.2)	0.1 M KOH	240	290	70	*J. Am. Chem. Soc.*, 2014, **136**, 13925-13931.
CoOOH (0.15)	1 M KOH	/	300	38	*Angew. Chem. Int. Ed.*, 2015, **54**, 8722-8727.
α-$Co(OH)_2$-Cl (0.2)	**1 M KOH**	**~240**	**~320**	**53**	**this work**
$CoSe_2$ (0.142)	0.1 M KOH	/	320	44	*J. Am. Chem. Soc.*, 2014, **136**, 15670-15675.
$Co_3Fe_7O_x$/NPC (0.36)	1 M KOH		328	31	*J. Mater. Chem. A*, 2016, **4**, 6048-6055.
crumpled graphene-CoO (0.7)	1 M KOH	/	340	71	*Energy Environ. Sci.*, 2014, **7**, 609-616.
$NiCo_{2.7}(OH)_x$	1 M KOH	250	350	65	*Adv. Energy Mater.*, 2015, **5**, 1402031.
CoMn-LDH (0.142)	1 M KOH	/	350	43	*J. Am. Chem. Soc.*, 2014, **136**, 16481-16484.
CoCo-NS (0.07)	1 M KOH	307	353	45	*Nat. Commun.*, 2014, **5**, 4477.
CoP/C	0.1 M KOH		360	66	*ACS Catal.*, 2015, **5**, 4066-4074.
$Ba_{0.5}Sr_{0.5}Co_{0.8}Fe_{0.2}O_{3-x}$	0.1 M KOH	314	~362	~48	*Science*, 2011, **134**, 1383-1385.
NG-$CoSe_2$ (0.2)	0.1 M KOH	293	366	40	*ACS Nano*, 2014, **8**, 3970-3978.
exfoliated NiCo LDH /carbon paper (0.08)	1 M KOH	/	367	40	*Nano Lett.*, 2015, **15**, 1421-1427.
reduced Co_3O_4 (0.136)	1 M KOH	290	~410	72	*Adv. Energy Mater.*, 2014, **4**, 1400696.
$SrNb_{0.1}Co_{0.7}Fe_{0.2}O_{3-\delta}$	0.1 M KOH	260	420	90	*Angew. Chem. Int. Ed.*, 2015, **54**, 1-6.
β-$Co(OH)_2$/Ti[a]	1 M KOH	280-290	500-510	/	*Chem. Mater.*, 2013, **25**, 1922-1926.
Au/mCo_3O_4	0.1 M KOH	300	650	46	*ChemSusChem*, 2014, **7**, 82-86.

[a] catalysts directly grown on the conductive substrate.

[b] The table was built by the column of the overpotential that reaches to the current density of 10 mA/cm^2 in a descending order.

[c] All the catalysts not mentioned the substrate were dropped on GCEs.

Table S3. TOFs of α-$Co(OH)_2$-Cl pretreated at different potentials (calculated from current density at η = 320 mV).

samples	***j* at η = 320 mV (mA/cm^2)**	**TOF at η = 320 mV (s^{-1})**
1.0 V	4.2	0.0051
1.3 V	10	0.0121